Prevention of resistive wall tearing mode major disruptions with feedback

H. R. Strauss[1, 1]

[1] HRS Fusion, West Orange, NJ 07052

Abstract

Resistive wall tearing modes (RWTM) can cause major disruptions. A signature of RWTMs is that the rational surface is sufficiently close to the wall to interact with it. For $(m, n) = (2, 1)$ modes, a RWTM requires normalized minor radius of the rational surface $\rho_{q2} \geq 0.75$, which can also be expressed as $q_{75} \leq 2$. Major disruptions can occur when the criterion is satisfied. This is confirmed in simulations and theory and in a DIII-D locked mode disruption database. The $q_{75} < 2$ criterion is valid at high β as well as at low β. A very important feature of RWTMs is that they can be feedback stabilized. If the ρ_{q2} criterion is not satisfied, or if the wall is ideally conducting, then the mode does not produce a major disruption, although it can produce a minor disruption. Feedback, or rotation of the mode at the wall by complex feedback, can emulate an ideal wall, preventing major disruptions. The ρ_{q2} criterion depends weakly on the wall radius. A simple geometric model of its dependence on wall radius is given.

1 Introduction

Resistive wall tearing modes (RWTM) can cause major disruptions. This is based on evidence from theory, simulations, and experimental data [1, 2, 3, 4, 5, 6]. For example, DIII-D locked mode shot 154576 [7] experienced a major disruption. Linear simulations [3] found the reconstructed equilibrium was stable with an ideal wall. and found a scaling of the linear growth rate with the wall penetration time. Nonlinear simulations found a complete thermal quench, and agreement with the experimental thermal quench (TQ) time and the amplitude of the perturbed magnetic field.

A signature of RWTMs is that the rational surface is sufficiently close to the wall to interact with it. For $(m, n) = (2, 1)$ modes, the required rational surface radius for a RWTM, normalized to the plasma radius, is $\rho_{q2} \geq 0.75$. This can also be expressed as the value of q at $\rho = 0.75$, $q_{75} < 2$. Major disruptions can occur when the criterion is satisfied. This is confirmed in simulations and theory. Experimentally, it is the disruption criterion in a DIII-D locked mode disruption database [8]. The database consists of tearing modes, nearly all having $\rho_{q2} \geq 0.75$, which cause disruptions. These are properties of RWTMs.

[1]Author to whom correspondence should be addressed: hank@hrsfusion.com

The $q_{75} < 2$ criterion is valid at high β as well as at low β. This is verified experimentally [9] as well as in simulations.

A very important feature of RWTMs is that they can be feedback stabilized. Without feedback, they can produce major disruptions when the $q_{75} < 2$ criterion is satisfied. This is verified experimentally and in simulations at low and high β.

The $\rho_{q2} \geq 0.75$ criterion applies to DIII-D, NSTX, and the MST - based model discussed below. For ITER, the requirement is $\rho_{q2} \geq 0.78$. The critical ρ_{q2} depends weakly on the normalized wall radius ρ_w.

The outline of the paper is as follows. The domain of instability of RWTMs in the (q_{75}, β) plane is presented qualitatively in Sec.2. Also shown is the $\rho_{q2} > 0.75$ database of DIII-D locked mode disruptions. The relevance of mode locking, precursors, edge cooling, and current contraction are discussed.

The computational model used for feedback and rotating wall is presented in Sec.3.

In Sec.4, simulations are presented of a sequence of equilibria in which major disruptions occur with a resistive wall, when $q_{75} < 2$.

Finite β experimental results in NSXT are presented in Sec.5.

Sec.6 shows simulations based on an NSTX intermediate β_N equilibrium.

The reason for the q_{75} criterion is analyzed in Sec.7. The critical value of ρ_{q2}/ρ_w is obtained.

A summary is provided in Sec.8.

2 RWTM parameter space

The expression $\rho_{q2} = 0.75$, can be written as $q_{75} = 2$, where $q_{75} = q(\rho = .75)$, which is useful to represent the RWTM unstable parameter space. Fig.1(a) gives a schematic parameter space (q_{75}, β) of resistive wall modes (RWM) and RWTMs with $\rho_w = 1.2$. The RWTM is unstable for $q_{75} \leq 2$, indicated by a vertical line, as shown in the following.

The RWM β limit is approximately the Troyon [10] β_N limit of an external kink interacting with a resistive wall. The RWTM is unstable below the RWM limit [11, 12]. The starred points in Fig.1(a) correspond to low and high β examples in Sec.4, Sec.5, and Sec.6. The point at $q_{75} = 1.8$ is from DIII-D [3, 6]. Both low and high β RWTM and RWM can be limited to minor disruptions by feedback, rotation, or an ideal wall. Locking with resistive wall and without feedback or rotation allows a major disruption.

Fig.1(b) shows a database of DIII-D disruptivity [8] which depends on ρ_{q2}. The onset is $\rho_{q2} = .75$ or $q_{75} = 2$.

The disruptions occur for locked modes. Mode locking means that toroidal rotation stops, destabilizing tearing modes [7, 13]. Sheared rotation stabilizes tearing modes [15, 14, 16], including RWTMs [17, 18, 19].

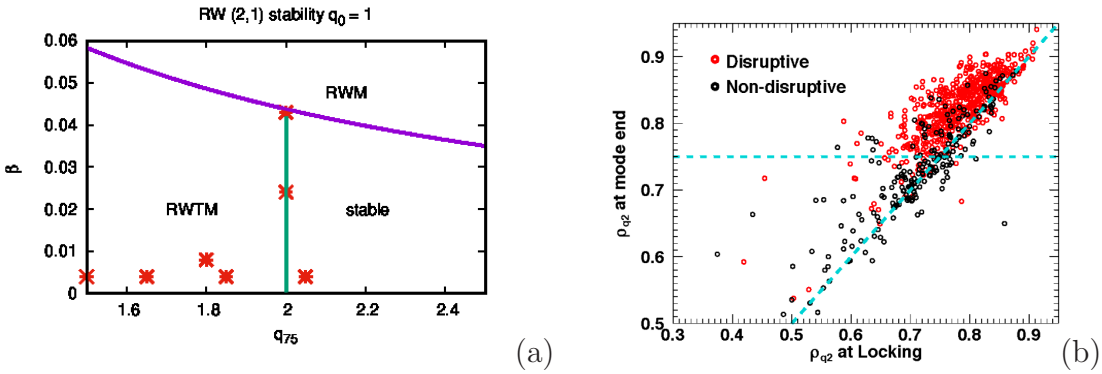

Figure 1: *(a) Schematic diagram of RWM and RWTM stability in* (q_{75}, β) *space. The vertical line at* $q_{75} = 2$ *is the RWTM stability boundary. (b) Disruptivity in a DIII-D locked mode disruption database. Reproduced from [8] with IAEA permission.*

Fig.1(b) also shows that ρ_{q2} tends to increase between mode locking and the disruption. The diagonal line shows unchanged ρ_{q2}. The profiles evolve to reduce the edge temperature and current density [20, 21]. This could be produced by edge cooling, which causes current contraction and increase of ρ_{q2}, as in Fig.5(a).

A current contraction model [5] is discussed in Sec.7. Current contraction is caused by edge cooling, which in turn can have several causes. One possible cause is overlapping tearing modes in the edge region, called a $T_{e,q2}$ collapse [7]. Another possibility is resistive ballooning turbulence, proposed as an explanation of the Greenwald density limit [22]. Another possible cause of edge cooling is impurity radiation [23]. The edge radiation might be raised by increasing the plasma density [24]. The impurities might be introduced purposefully, as in massive gas injection [25, 26], or accidentally, as UFOs, pieces of plasma facing tiles falling into the plasma. It should be noted that the MGI simulations used an ideal wall boundary condition. These edge cooling mechanisms have been called causes of disruptions, but they are really precursors, which can destabilize a RWTM.

3 Feedback

Active feedback and wall rotation can make the wall effectively ideal and suppress RWTM major disruptions. There have been extensive theoretical [27, 28, 29] and experimental studies of feedback stabilization [30, 31, 9]. To model feedback, consider the magnetic diffusion equation at a thin resistive wall [1, 3, 6, 17]

$$\frac{\partial \psi_w}{\partial t} = \frac{r_w}{\tau_w}(\psi'_{vac} - \psi'_p + \psi'_f) \tag{1}$$

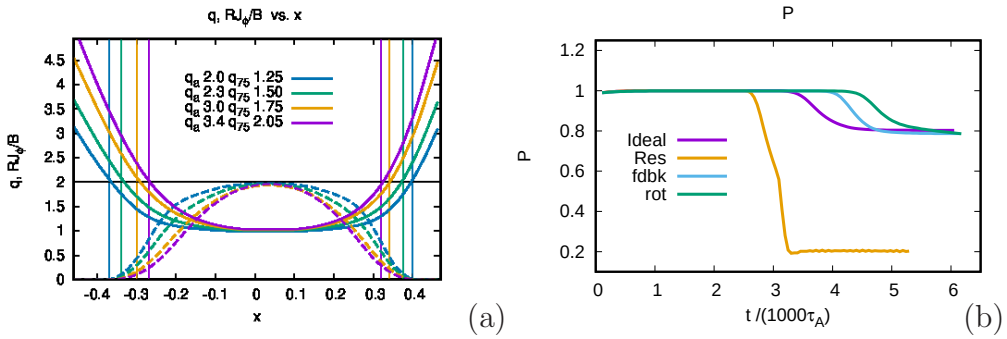

Figure 2: *(a) q and RJ_ϕ profiles of model equilibria as a function of radius $x = R - R_0$ for model equilibria with $q_a = 2.0, 2.3, 3, 3.4$. All but $q_a = 3.4$ have $q_{75} < 2$. (b) time histories of case $q_a = 3$ with ideal, resistive, feedback, and rotating wall boundary conditions. In all but the resistive wall case, only a minor disruption occurs.*

where ψ_w is the magnetic potential at the wall, ψ'_p is its radial derivative on the plasma side of the wall, $\tau_w = \mu_0 r_w \delta_w / \eta_w$, η_w, δ_w are wall resistivity and thickness, $r_w = R_w - R_0$, the difference of wall major radius and magnetic axis, and $\psi'_{vac} \approx -m\psi_w / r_w$ is the radial derivative of ψ_w on the vacuum side of the wall. An external feedback vacuum field ψ'_f is added with

$$\psi'_f = -D\frac{\tau_w}{r_w}\left(\gamma_w \psi_w + \Omega_w \frac{\partial \psi_w}{\partial \phi}\right) - hF\psi'_p \tag{2}$$

where the γ_w and Ω_w terms model complex normal gain, h models transverse gain, $D(\theta, \psi_w)$, $F(\theta, \psi_w)$ are screening functions of poloidal and toroidal angle of the wall, modeling the location of the sensors. For now, take $D = F = 1$. They could be taken non zero in future numerical studies, and might affect detailed predictions of the modeling. Only toroidal mode number $n = 1$ is included in ψ'_f. The γ_w and Ω_w terms model saddle coils which sense $b_n \propto \psi'_{vac}$ while h models probes which sense transverse perturbed magnetic field $b_l \propto \psi'_p$. Then (1) can be expressed

$$\frac{\partial \psi_w}{\partial t} = \frac{r_w}{\tau_w}[(\psi'_{vac} - (1+h)\psi'_p] - \gamma_w \psi_w - \Omega_w \frac{\partial \psi_w}{\partial \phi}. \tag{3}$$

The γ_w term causes damping of ψ_w and the Ω_w term models a rotating wall boundary condition [29, 32]. The relative rotation of the rational surface in the plasma and the wall can stabilize a RWTM [18, 19].

In the simulations in this paper, only γ_w and Ω_w are used, and are constant in time. Simulations with h give similar results [6]. More advanced experimental methods vary the feedback gain in time [9]. The goal here is to demonstrate that feedback or wall rotation can prevent major disruptions, although it can permit minor disruptions.

4 Low β RWTM disruptions

Simulations were performed with M3D [33] for a sequence of modified MST equilibria [5, 6]. Here the results are extended by including simulations with feedback and wall rotation, as discussed in Sec.3. The simulations had parameters: Lundquist number $S = 10^5$, wall Lundquist number $S_w = \tau_w/\tau_A = 10^3$, where τ_w is the wall penetration time defined in Sec.3, $\tau_A = R/v_A$ is the Alfvén time, R is major radius, v_A is Alfvén velocity, and parallel thermal conductivity $\kappa_\parallel = 10R^2/\tau_A$. The simulation had 16 toroidal planes. In MST [4], the wall time is much longer than the pulse time, so the wall is effectively ideal. Here and in [5], the resistive wall time is shortened, more like in DIII-D and other tokamaks.

Fig.2 shows $q(x)$ and $RJ_\phi(x)$ profiles for a sequence of modified MST equilibria [5] with $\rho_w = 1.2$. The radius $x = R - R_0$ is measured from the magnetic axis along the major radius. The normalized minor radius $\rho = x/a \geq 0$, where a is the plasma radius.

The profiles have $q_0 = 1$ and edge $q_a = 2, 2.3, 3, 3.4$. For $q_a \leq 3$, $q_{75} < 2$, so the equilibria are unstable to RWTMs. The case $q_a = 3.4$ is RWTM marginally stable. Nonlinear simulations were initialized with these equilibria. It was shown [5] that with an ideal wall, all the equilibria are unstable only to minor disruptions. For $q_a \leq 3$, $q_{75} < 2$, with a resistive wall, major disruptions occur. If $q_a = 3.4$, $q_{75} > 2$, and the wall is resistive, the disruption is minor.

The particular case $q_a = 3$, $q_{75} = 1.75$ is considered in more detail. Fig.2 (b) shows time histories of thermal energy, the integrated pressure P for the case $q_a = 3$, with ideal wall, resistive wall, feedback, and wall rotation. A major disruption occurs for a resistive wall. All the other boundary conditions give only minor disruptions. Fig.3 shows contours of pressure and perturbed magnetic field in nonlinear simulations

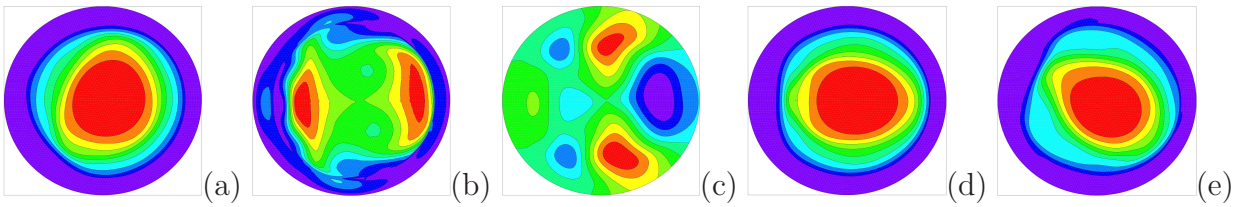

Figure 3: *Pressure p contours in nonlinear simulation of the q_a case for (a) ideal wall, (b) resistive wall, (c) perturbed magnetic flux ψ corresponding to case (b), (d) feedback stabilization, (e) rotating wall. Fig.3(a),(b) reproduced from [5] with AIP permission.*

corresponding to the time histories in Fig.2, including feedback and wall rotation. The simulations demonstrate that ideal wall, feedback, and rotating wall limit growth of tearing mode. A resistive wall (or no wall) allows a tearing mode to reach much larger amplitude than an ideal wall, or similar boundary conditions. Contours of pressure p are shown near the last times in the history plot Fig.2. The contour plots correspond

to boundary conditions (a) ideal wall, (b) resistive wall with no rotation, (d) feedback, and (e) edge rotation. Boundary conditions (d) and (e) are similar to (a), with small perturbations and only minor disruptions. In (c), perturbed magnetic flux ψ contours correspond to the pressure contours in (b). The perturbed flux is relevant to the anaysis of ρ_{q2} in Sec.7.

The feedback case in Fig.2 (b) and Fig.3 (d) has parameter $\gamma_w \tau_A = 0.02$. The rotation example in Fig.2 (b) and Fig.3 (e) has $\Omega_w \tau_A = 0.05$. These values would be expected to decrease with longer RWTM growth time.

5 High β NSTX RWTM

RWM and RWTM can be found together at high β. Both can be feedback stabilized. Fig.4 gives an NSTX example [9] , with $\beta_N > 4$, above the no wall limit. The feedback

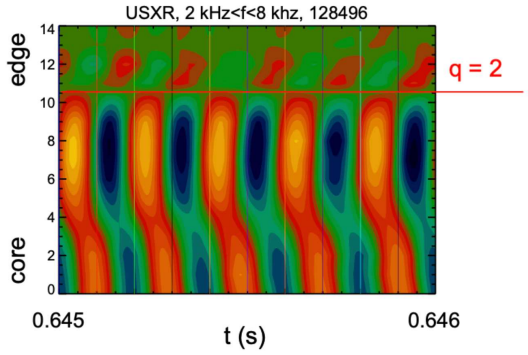

Figure 4: *feedback stabilized* $(2,1)$ *RWTM. The RWTM can be identified by its phase inversion at* $\rho_{q2} = 0.75$. *Reproduced from [9] with IAEA permission.*

is with complex gain, which can vary in time as the modes grow. Time dependent soft X ray data shows radial mode structure. Initially a locked RWM is stabilized by feedback. It then spins up and converts to a stabilized external kink. It then becomes in Fig.4 a feedback stabilized $(2,1)$ RWTM. The RWTM can be identified by its phase inversion in soft X ray emission at $\rho_{q2} \approx 0.75$. It is a RWTM because it is close enough to the wall to be affected by the feedback imposed at the wall. This suggests that initially $q_0 > 1$ on axis and $\rho_{q2} < 0.75$. Resistive evolution causes current profile peaking and decreases q_0 on axis, pushing $\rho_{q2} \geq 0.75$. An example is seen in the simulations of Sec.6.

A similar phenomenon is seen was seen in DIII-D [31]. After an ELM, a tearing mode developed in shot 131753 with $\rho_{q2} \approx 0.75$, with growth time $10ms$, when the toroidal velocity at $\rho_{75} \approx 0$. The mode caused a major disruption, in which the ratio of initial to final β dropped from 1 to less than 0.25. It is possible that the mode was

a neoclassical tearing mode (NTM) that was triggered by an ELM, but it was also sufficiently close to the wall to be a RWTM. It might be noted that modeled NTMs do not reach large amplitude [34] like RWTMs.

It appears that RWTMs were observed and feedback stabilized in KSTAR [35]. A simulation based on a KSTAR equilibrium reconstruction with $\beta_N = 3.7$ showed a $(2,1)$ mode with magnetic perturbations extending through the wall, evidently a RWTM although not identified as such [35].

6 High β NSTX simulations

Simulations were done with M3D of modified NSTX equilibrium reconstructions of shot 109070. The simulation parameters were the same as in Sec.4. An example is given in Fig.5 with $\beta_N = 3$. Fig.5(a) gives midplane $q(x)$ profiles, $x = R - R_0$, at

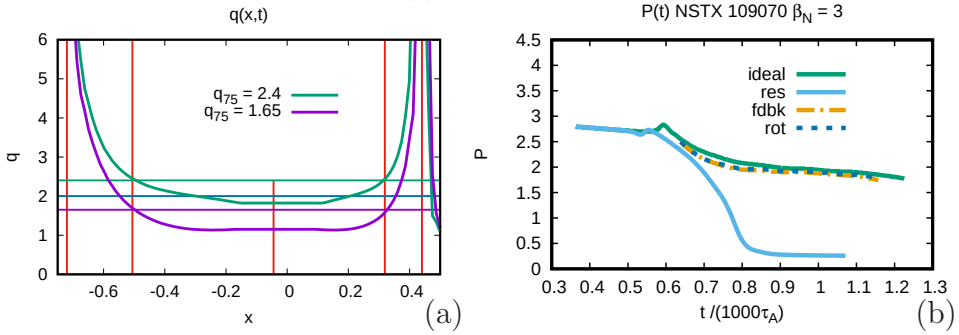

Figure 5: *(a) $q(x)$ profiles with evolution to RWTM instability. (b) Time histories of thermal energy P with different boundary conditions: ideal wall, resistive wall, feedback, and rotating wall.*

nearly the initial time, when $q_0 = 1.3$ and $q_{75} = 2.4$. It appears stable to a $(2,1)$ and $(3,1)$ mode. The initial state was not in resistive equilibrium. The plasma was allowed to evolve resistively, with total current held constant in time. This caused the current to contract until $q_0 \approx 1$, and $q_{75} = 1.65$. The equilibrium was then RWTM unstable to a $(2,1)$ mode. Fig.5 (b) shows time histories of thermal energy P with different boundary conditions: ideal wall, resistive wall, feedback, and wall rotation. Only the case with resistive wall without feedback or wall rotation has a major disruption. The other cases all have minor disruptions. Fig.6 shows contours of pressure with (a) ideal wall; (b) resistive wall; (d) feedback; (e) rotating wall. A major disruption occurs only with a locked resistive wall. The pressure contours have a large perturbation, as in Fig.3. Fig.6(c) shows $n > 1$ contours of ψ. The perturbations are large lobes which penetrate the wall.

The feedback example in Fig.5(b), Fig.6 (d) has parameter $\gamma_w \tau_A = 0.05$. The rotation example in Fig.5(b), Fig.6 (e) has $\Omega \tau_A = 0.05$.

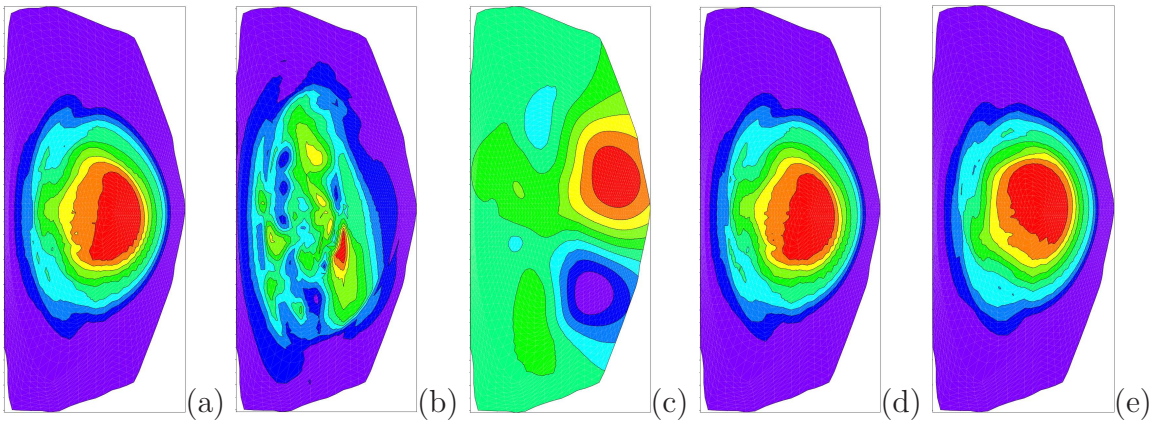

Figure 6: *Contours of pressure near the end of the time histories in Fig.5(b). with (a) ideal wall; (b) resistive wall; (c) perturbed magnetic flux of resistive case (b); (d) magnetic feedback; (e) rotating wall.*

At high β, there are also RWMs, resistive wall external kink modes. Evidently they can also be stabilized by feedback [9] as mentioned in Sec.5. Simulations of RWMs will be presented elsewhere.

7 Dependence of ρ_{q2} on wall position

The critical ρ_{q2} depends on normalized wall radius ρ_w. The critical value $\rho_{q2} = .75$ occurs for $\rho_w = 1.2$, as in DIII-D, NSTX, and the MST model in Sec.4. This can be obtained from a linear model [5] using modified [36] equilibrium profiles with current density $j(\rho) = 0$ for $\rho > \rho_c$, with $j(\rho) = (2/q_0)(1+\rho^{2\nu})^{-(1+1/\nu)} - c_r$ with $c_r = (1+\rho_c^{2\nu})^{-(1+1/\nu)}$, and $q(0) = 1$. Contraction of the current profile is modeled with the current cutoff radius ρ_c. The profile peakedness parameter ν is determined by ρ_c and q_a. Linear ideal MHD equations for perturbed magnetic flux ψ with mode number $(2,1)$ were solved in a periodic cylinder. An example is given in Fig.7(a), with $q_a = 2.5$, $\rho_c = 0.7$. The normalized $q = 2$ radius is $\rho_{q2} = 0.9$. Solutions of $\psi(\rho)$ are given for an ideal wall boundary condition $\psi(\rho_w) = 0$ and a no wall boundary condition $d\psi(\rho_w)/d\rho = -2\psi(\rho_w)/\rho_w$. The stability parameter $\Delta' = [\psi'(\rho_{q2+}) - \psi'(\rho_{q2-})]/\psi(\rho_{q2})$ is calculated at ρ_{q2} for ideal and no wall boundary conditions. For an ideal wall, $\Delta' = \Delta_i = -0.26$, while for no wall, $\Delta' = \Delta_n = 1.38$. This is an unstable RWTM. The boundary condition causes $\Delta_n > \Delta_i$ [1, 17] as can be seen in Fig.7(a). In Fig.7(b) are plotted curves $\rho_{ci}(\rho_{q2}, \rho_w)$ for $\Delta_i = 0$ with ideal wall and $\rho_{cn}(\rho_{q2})$ with $\Delta_n = 0$ for no wall. Four ρ_{ci} curves are plotted, for $\rho_w = 1.1, 1.2, 1.3, 1.5$. There is only one $\rho_{cn}(\rho_{q2})$ curve, since it does not depend on ρ_w. The RWTM is unstable for $\rho_{ci} \geq \rho_c \geq \rho_{cn}$. The unstable region is between the dotted curve for given $\rho_{ci}(\rho_w)$ and the solid curve

ρ_{cn}. The onset condition for a RWTM is $\rho_{ci} = \rho_{cn}$. All the curves satisfy $\rho_{q2} > \rho_c$, with the current contracted within ρ_{q2}, so that $q_a = 2/\rho_{q2}^2$. For $\rho_w = 1.2$, $\rho_{q2} = 0.75$

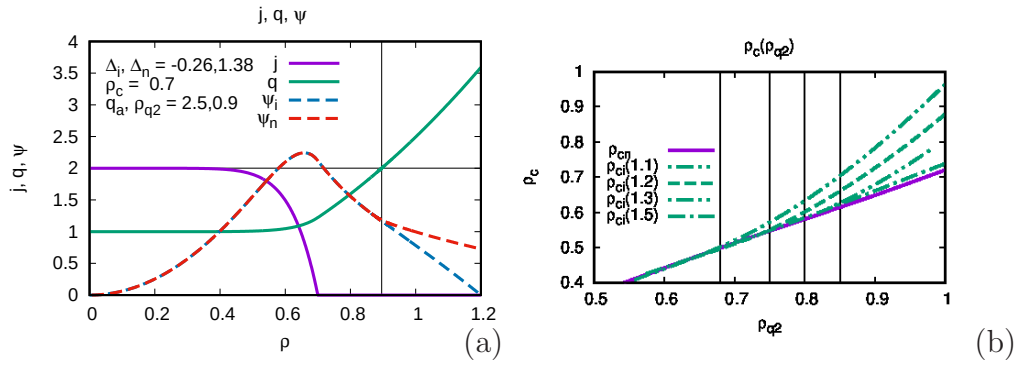

Figure 7: *(a) ψ, j, and q, with ψ for ideal (ψ_i) and no wall (ψ_n). (b) Curves of $\rho_{ci}(\rho_{q2})$, and $\rho_{cn}(\rho_{q2})$ for $\rho_w = 1.1, 1.2, 1.3, 1.5$.*

as in Fig.1(b). Fig.7(b) gives a relation between ρ_{q2} and ρ_w, shown in Fig.8(a), where

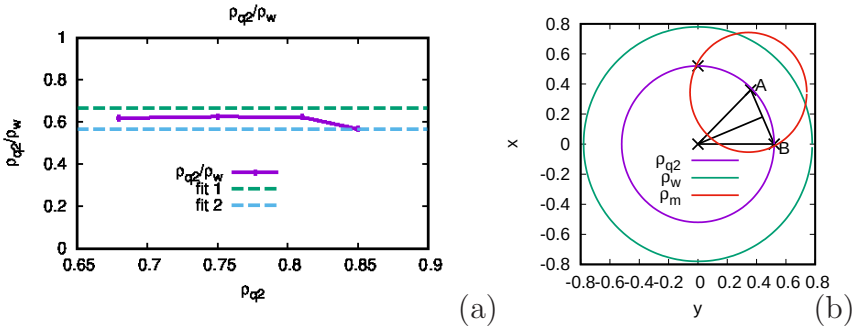

Figure 8: *(a) ρ_{q2}/ρ_w is nearly constant, for $\rho_w > 1.3$. (b) model of wall interaction of $(m, n) = (2, 1)$ mode.*

ρ_{q2}/ρ_w is constant, up to a critical value of $\rho_w > 1.3$. For $\rho_w > 1.5$, the mode becomes a no wall tearing mode, and does not interact with the wall.

A simple way to estimate ρ_{q2}/ρ_w is to require that the tearing mode magnetic perturbation extend to the wall, $\rho_w = \rho_{q2} + 1/(k_\perp a)$, where $k_\perp a = m/\rho_{q2}$, m is the poloidal mode number, and a is the wall radius. Then

$$\rho_{q2} = \rho_w/(1 + 1/m). \tag{4}$$

This is labelled "fit 1" in Fig.8(b). A lower bound is obtained by noting that the magnetic $n \geq 1$ perturbations shown in Fig.3(c) and Fig.6(c) are lobes which extend into the wall. In Fig.8(b), an (m, n) lobe is modeled as dividing the contour $\rho = \rho_{q2}$ into

$2m$ arcs with ends at angles $0, \pi/m, \ldots$ The midpoints are at $\pi/(2m), \ldots$. A chord of length $\rho_m = 2\sin(\pi/4m)\rho_{q2}$ can be drawn connecting the midpoint of the arc labelled "A" to the intersection of the arc with the x axis at "B". This is the radius of a circle with origin at "A", shown in Fig.8(b). It models a lobe of a (m, n) mode structure. The radius of the circle must be large enough to intersect the wall, such that $\rho_w \leq \rho_{q2} + \rho_m$. This can be expressed as (4) with $2\sin(\pi/(4m))$ replacing $1/m$. This is labelled "fit 2" in Fig.7(a). The calculated line in Fig.8(a) intersects the fit at $\rho_{q2} = 0.85$, where according to Fig.7(b), $\rho_w = 1.5$. This suggests that for larger ρ_w, the wall is too far away to interact with the mode.

8 Summary

To summarize, resistive wall tearing modes (RWTM) can cause cause major disruptions. A signature of RWTMs is that the rational surface is sufficiently close to the wall to interact with it. For $(m, n) = (2, 1)$ modes, the rational surface radius of the $q = 2$ surface, normalized to the plasma minor radius, is $\rho_{q2} > 0.75$, for normalized wall radius $\rho_w = 1.2$. This can also be expressed as the value of q at $\rho_{q2} = 0.75$, $q_{75} < 2$. The ρ_{q2} criterion is weakly dependent on ρ_w. The domain of instability of RWTMs in the (q_{75}, β) plane was presented qualitatively. The $\rho_{q2} > 0.75$ criterion was found in a DIII-D locked mode disruption database. The importance of mode locking and disruption precursors was discussed.

A very important feature of RWTMs is that they can be stabilized by feedback and wall rotation. The computational model used for feedback and rotating wall was discussed. Stabilization was verified in simulations of a sequence of low β equilibria. It was shown that when the wall is resistive and the q_{75} criterion is satisfied, the saturated mode amplitude is large.

At high β, feedback stabilized $(2, 1)$ modes were observed in NSTX with $\rho_{q2} \approx 0.75$, indicating wall interaction, implying a RWTM. Simulations were performed using modified NSTX equilibria at moderate $\beta_N = 3$, which satisfied $q_{75} < 2$, and produced major disruptions with a resistive wall, minor disruptions with an ideal wall, feedback, or rotating wall.

The ρ_{q2} criterion was analyzed in model simulations, and a simple geometric model of its dependence on ρ_w was given. The ratio ρ_{q2}/ρ_w is nearly constant up to a critical $\rho_w > 1.3$. For $\rho_w > 1.5$, the wall is too far away for a RWTM and the mode becomes a no wall tearing mode.

In conclusion, $(m, n) = (2, 1)$ RWTMs satisfy a ρ_{q2} condition. The boundary conditions at the wall can prevent a major disruption. With an ideally conducting wall, tearing modes produce only minor disruptions. Feedback and rotating wall boundary conditions act like an ideal wall. This could potentially eliminate disruptions from

tokamaks, greatly enhancing the prospects of magnetic fusion.

Acknowledgement Thanks to S. Sabbagh for pointing out the possible RWTM in [9]. This work was supported by U.S. D.O.E. grant DE-SC0020127.

References

[1] H. Strauss and JET Contributors, Effect of Resistive Wall on Thermal Quench in JET Disruptions, Phys. Plasmas **28**, 032501 (2021)

[2] H. Strauss, Thermal quench in ITER disruptions, Phys. Plasmas **28** 072507 (2021)

[3] H. Strauss, B. C. Lyons, M. Knolker, Locked mode disruptions in DIII-D and application to ITER, Phys. Plasmas **29** 112508 (2022);

[4] H. R. Strauss, B. E. Chapman, N. C. Hurst, MST Resistive Wall Tearing Mode Simulations, Plasma Phys. Control. Fusion **65** 084002 (2023).

[5] H. R. Strauss, Models of resistive wall tearing mode disruptions, Phys. Plasmas 30, 112507 (2023); doi:10.1063/5.0172375

[6] H. R.Strauss, B. E. Chapman, B. C. Lyons, Resistive Wall Tearing Mode Disruptions, Nucl. Fusion **64** 106037 (2024); doi:10.1088/1741-4326/ad7272

[7] R. Sweeney, W. Choi, M. Austin, M. Brookman, V. Izzo, M. Knolker, R.J. La Haye, A. Leonard, E. Strait, F.A. Volpe and The DIII-D Team, Relationship between locked modes and thermal quenches in DIII-D, Nucl. Fusion **58**, 056022 (2018)

[8] R. Sweeney, W. Choi, R. J. La Haye, S. Mao, K. E. J. Olofsson, F. A. Volpe, and the DIII-D Team, Statistical analysis of m/n = 2/1 locked and quasi - stationary modes with rotating precursors in DIII-D, Nucl. Fusion 57 0160192 (2017).

[9] S. A. Sabbagh, S.P. Gerhardt, J.E. Menard, R. Betti, D.A. Gates, B. Hu, O.N. Katsuro-Hopkins, B.P. LeBlanc, F.M. Levinton, J. Manickam, K. Tritz and H. Yuh, Advances in global MHD mode stabilization research on NSTX, Nucl. Fusion **50** 025020 (2010).

[10] F. Troyon, A.Roy, W.A.Cooper, F.Yasseen, A.Tumbull, Beta limit in tokamaks: experimental and computational status, Plasma Physics and Controlled Fusion textbf30, 1597 (1988).

[11] R. Betti, Beta limits for the n = 1 mode in rotating - toroidal - resistive plasmas surrounded by a resistive wall, Phys. Plasmas 5, 3615 (1998).

[12] H. R. Strauss, Linjin Zheng, M. Kotschenreuther, W.Park, S. Jardin, J. Breslau, A.Pletzer, R. Paccagnella, L. Sugiyama, M. Chu, M. Chance, A. Turnbull, Halo Current and Resistive Wall Simulations of ITER, paper TH/2 - 2, 20th IAEA Fusion Energy Conference 2004, Villamora, Portugal (2004).

[13] S.N. Gerasimov, P. Abreu, G. Artaserse, M. Baruzzo, P. Buratti, I.S. Carvalho, I.H. Coffey, E. De La Luna, T.C. Hender, R.B. Henriques, R. Felton, S. Jachmich, U. Kruezi, P.J. Lomas, P. McCullen, M. Maslov, E. Matveeva, S. Moradi, L. Piron1, F.G. Rimini, W. Schippers, C. Stuart, G. Szepesi, M. Tsalas, D. Valcarcel, L.E. Zakharov and JET Contributors, Overview of disruptions with JET-ILW, Nucl. Fusion **60** 066028 (2020).

[14] S. Wang, Z. W. Ma, Influence of toroidal rotation on resistive tearing modes in tokamaks, Phys. Plasmas 22, 122504 (2015); doi:10.1063/1.4936977

[15] R. Coelho, E. Lazzaro, Effect of sheared equilibrium plasma rotation on the classical tearing mode in a cylindrical geometry, Phys. Plasmas 14, 012101 (2007)

[16] H. R. Strauss, Rotational stabilization of drift tearing modes, Phys. Fluids **B 4** 3 (1992); doi:10.1063/1.860448

[17] J. A. Finn, Resistive wall stabilization of kink and tearing modes, Phys. Plasmas 2, 198 (1995)

[18] C.G. Gimblett, On free boundary instabilities induced by a resistive wall, Nucl. Fusion 26, 617 (1986)

[19] A. Bondeson and M. Persson, Stabilization by resistive walls and q-limit disruptions in tokamaks, Nucl. Fusion 28, 1887 (1988)

[20] F.C. Schuller, Disruptions in tokamaks, Plasma Phys. Controlled Fusion **37**, A135 (1995).

[21] J.A. Wesson, R.D. Gill, M. Hugon, F.C. Schuller, J.A. Snipes, D.J. Ward, D.V. Bartlett, D.J. Campbell, P.A. Duperrex, A.W. Edwards, R.S. Granetz, N.A.O. Gottardi, T.C. Hender, E. Lazzaro, P.J. Lomas, N. Lopes Cardozo, K. F. Mast, M.F.F. Nave, N.A. Salmon, P. Smeulders, P.R. Thomas, B.J.D. Tubbing, M.F. Turner, A. Weller, Disruptions in JET, Nucl. Fusion **29** 641 (1989).

[22] M. Giacomin, A. Pau, P. Ricci, O. Sauter, T. Eich, the ASDEX Upgrade team, JET Contributors, and the TCV team, First-Principles Density Limit Scaling in Tokamaks Based on Edge Turbulent Transport and Implications for ITER Phys. Rev. Lett. 128, 185003 (2022)

[23] G. Pucella, P. Buratti, E. Giovannozzi, E. Alessi, F. Auriemma, D. Brunetti, D. R. Ferreira, M. Baruzzo, D. Frigione, L. Garzotti, E. Joffrin, E. Lerche, P. J. Lomas, S. Nowak, L. Piron, F. Rimini, C. Sozzi, D. Van Eester, and JET Contributors, Tearing modes in plasma termination on JET: the role of temperature hollowing and edge cooling, Nucl. Fusion **61** 046020 (2021)

[24] D. A. Gates, D. P. Brennan, L. Delgado-Aparicio, and R. B. White, The tokamak density limit: A thermo- resistive disruption mechanism, Phys. Plasmas 22, 060701 (2015); https://doi.org/10.1063/1.4922472

[25] V. A. Izzo, D. G. Whyte, R. S. Granetz, P. B. Parks, E. M. Hollmann, L. L. Lao, J. C. Wesley, Magnetohydrodynamic simulations of massive gas injection int Alcator C - Mod and DIII-D plasmas, Phys. Plasmas **15**, 056109 (2008).

[26] E. Nardon, A. Fil, M. Hoelzl, G. Huijsmans and JET contributors, Progress in understanding disruptions triggered by massive gas injection via 3D non-linear MHD modelling with JOREK, Plasma Phys. Control. Fusion **59** 014006 (2017).

[27] A. Bondeson, Yueqiang Liu, D. Gregoratto, Y. Gribov and V.D. Pustovitov, Active control of resistive wall modes in the large-aspect-ratio tokamak, Nucl. Fusion 42 (2002) 768–779

[28] Yuling He, Yueqiang Liu, Xu Yang, Guoliang Xia, Li Li, Active control of resistive wall mode via modification of external tearing index, Physics of Plasmas 28, 012504 (2021)

[29] D. P. Brennan, J. M. Finn, Control of linear modes in cylindrical resistive magnetohydrodynamics with a resistive wall, plasma rotation, and complex gain, Phys. Plasmas **21**, 102507 (2014).

[30] A.M. Garofalo, G.L. Jackson, R.J. La Haye, M. Okabayashi, H. Reimerdes, E.J. Strait, J.R. Ferron, R.J. Groebner, Y. In, M.J. Lanctot, G. Matsunaga, G.A. Navratil, W.M. Solomon, H. Takahashi, M. Takechi, A.D. Turnbull and the DIII-D Team, Stability and control of resistive wall modes in high beta, low rotation DIII-D plasmas, Nucl. Fusion **47** 1121–1130 (2007).

[31] M. Okabayashi, I.N. Bogatu, M.S. Chance, M.S. Chu, A.M. Garofalo, Y. In, G.L. Jackson, R.J. La Haye, M.J. Lanctot, J. Manickam, L. Marrelli, P. Martin, G.A. Navratil, H. Reimerdes, E.J. Strait, H. Takahashi, A.S. Welander, T. Bolzonella, R.V. Budny, J.S. Kim, R. Hatcher, Y.Q. Liu and T.C. Luce, Comprehensive control of resistive wall modes in DIII-D advanced tokamak plasmas, Nucl. Fusion 49 (2009) 125003.

[32] M. Okabayashi, P. Zanca, E.J. Strait, A.M. Garofalo, J.M. Hanson, Y. In5, R.J. La Haye, L. Marrelli, P. Martin, R. Paccagnella, C. Paz-Soldan, P. Piovesan, C. Piron, L. Piron, D. Shiraki, F.A. Volpe and The DIII-D and RFX-mod Teams, Avoidance of tearing mode locking with electro-magnetic torque introduced by feedback-based mode rotation control in DIII-D and RFX-mod, Nuclear Fusion 57, 016035 (2017)

[33] W. Park, E. Belova, G. Y. Fu, X. Tang, H. R. Strauss, L. E. Sugiyama, Plasma Simulation Studies using Multilevel Physics Models, Phys. Plasmas 6, 1796 (1999).

[34] R.J. La Haye, C. Chrystal , E.J. Strait , J.D. Callen, C.C. Hegna, E.C. Howell , M. Okabayashi and R.S. Wilcox, Disruptive neoclassical tearing mode seeding in DIII-D with implications for ITER, Nucl. Fusion 62 056017 (2022).

[35] Y.S. Park, S.A. Sabbagh, J.H. Ahn, B.H. Park, H.S. Kim, J.W. Berkery, J.M. Bialek, Y. Jiang, J.G. Bak, A.H. Glasser, J.S. Kang, J. Lee, H.S. Han, S.H. Hahn, Y.M. Jeon, J.G. Kwak, H.K. Park, Z.R. Wang, J.-K. Park, N.M. Ferraro and S.W. Yoon, Analysis of MHD stability and active mode control on KSTAR for high confinement, disruption-free plasma, Nucl. Fusion **60** 056007 (2020); doi:10.1088/1741-4326/ab79ca

[36] H. P. Furth, P. H. Rutherford, and H. Selberg, Tearing mode in the cylindrical tokamak, Physics of Fluids 16, 1054 (1973)